Cathodoluminescence investigation of silicon nanowires fabricated by thermal evaporation of SiO

© G. Jia[†*¶], T. Arguirov[†*¶¶], M. Kittler[†*], Z. Su[‡], D. Yang[•], J. Sha[‡]

[†] IHP microelectronics, Im Technologiepark 25,
15236 Frankfurt (Oder), Germany
[*] IHB/BTU Joint Lab, Postfach 101344,
03013 Cottbus, Germany
[‡] Department of Physics, Zhejiang University,
Hangzhou 310027, P.R. China
[•] State Key Lab of Silicon Materials, Zhejiang University,
Hangzhou 310027, P.R. China

(Получена 12 сентября 2006 г. Принята к печати 3 октября 2006 г.)

Silicon nanowire samples fabricated by thermal evaporation of SiO powder were investigated by cathodoluminescence. Three main bands were found at low temperatures, namely peak *1* at about 620–650 nm (2.0–1.91 eV), peak *2* at 920 nm (1.35 eV) and peak *3* at 1280 nm (0.97 eV). An additional broad band (peak *4*) in the infrared region with its maximum at ∼ 1570 nm (0.79 eV) appears at room temperature. The origins of the emission bands are discussed.

PACS: 78.60.Hk, 78.67.Lt

1. Introduction

Light emission from bulk silicon is generally difficult due to the indirect band gap. In the past few decades, great efforts have been made to investigate luminescence of silicon and to increase its quantum efficiency. The interest is driven by the need for optoelectronics and its compatibility with silicon technology. Infrared emission with energies lower than the band gap of silicon attracted great attentions for its transparent property in the silicon material, especially at wavelength around 1550 nm, the 1550 nm emission is also in correspondence with the low loss of the silica based glass fibers for optical communications.

Near-infrared emission around 1550 nm was found in silicon based materials, for example, in the dislocated silicon [1], in erbium doped silicon [2]. β-FeSi$_2$ also shows efficient emission in this spectral range [3]. In low-dimensional silicon, which typically shows visible light emission, the 1550 nm emission band was seldom reported.

Low-dimensional silicon structures, especially silicon nanowires (SiNWs) belong to the most investigated materials due to their fascinating luminescence properties [4]. The rapid progress in nanowire technology [5–10] renders SiNWs increasingly a potential use as building blocks of nanoelectronics, although some problems such as reproducibility and reliability ets. still remain. Recently, SiNWs based field effect transistors (FETs) have been realized with parameters better than those of state-of-the-art planar silicon devices [10,11].

2. Experimental

The SiNWs were fabricated by evaporating SiO powder on *p*-type (111) silicon substrates with the resistivity of about 0.001 Ω · cm. The details of the fabrication method are described elsewhere [12].

With this method SiNWs with an average diameter of about 20 nm were produced and they typically consist of a crystalline silicon core covered by a Si oxide layer with a thickness up to half of the wire diameter [13]. The core of the SiNWs was found to consist of crystalline silicon with a high density of defects such as stacking faults as well as micro-twins and the Si oxide shell to be amorphous [14].

The SiNW samples were investigated using a Zeiss EVO 40 scanning electron microscope equipped with a Gatan MonoCL system and a Hamamatsu IR photomultiplier with a sensitivity range from 250 to 1700 nm. For the cathodoluminescence (CL) measurements the samples were fixed on the sample holder with a conductive adhesive double side tape and silver paint. The measurements were performed at an accelerating voltage of 7 kV. The samples were investigated between 77 and 300 K using a cold stage system. Special care was taken to correct the temperature-related drift of the sample position. This ensured that the CL spectra recorded at different temperatures originate from the same area of the sample studied. The sampled area during the CL measurements was typically $50\times50\,\mu$m and the beam current was about 50 nA. To keep electron beam induced damage as low as possible, the beam was blanked except for the time needed to record a spectrum or to take a micrograph. In particular, this was done during the time required to reach a new pre-set value of the sample temperature.

3. Results

Three main bands were detected in all samples at 77 K (Fig. 1), with their maxima positioned at about 620–650 nm (2.0–1.91 eV) (named peak *1*), 920 nm (1.35 eV) (peak *2*) and 1270 nm (0.97 eV) (peak *3*). Moreover, there is a small

---

[¶] E-mail: jiaguobi@tu-cottbus.de
[¶¶] E-mail: arguirov@tu-cottbus.de

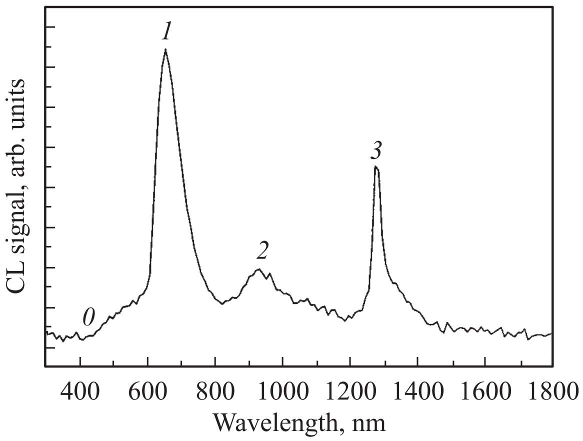

Figure 1. CL spectrum at liquid nitrogen temperature.

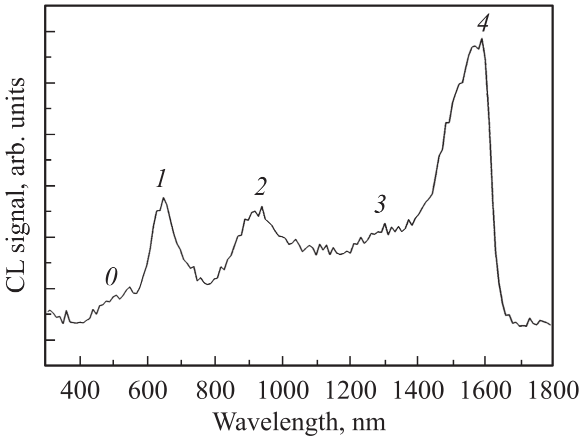

Figure 2. CL spectrum at room temperature.

shoulder at about 500 nm which is named peak *0*, see Fig. 1. At room temperature an additional peak around 1570 nm (0.79 eV) appears as shown in Fig. 2.

4. Discussion

Datails of these emission bands are shown in Fig. 3. The band around 500 nm is in fact at about 470 nm due to low sensitivity of the system at lower wavelength side. This band is a well known one from silica-based glass [15], but was also found in Si oxide/Si systems [16]. Its nature is related to oxygen deficient centers (ODCs) in the Si oxide matrix [17], detailed investigations indicated that this band may also have different origins [18]. The exact peak position of this band depends on the charge states and the nature of the defects [15]. The origin of the red emission of peak *1* in silicon nanostructures is still under strong debate. Firstly, there exists always a Si oxide film on the surface and this emission may originate from the nonbridging oxygen–hole centers (NBOHC) in the Si oxide matrix [19]. Secondly, if the dimension of the nanostructure decreases down to a few nanometers, the quantum confinement effect will play an important role in the formation of the red emission [20]. In our case the diameter of the SiNWs is too large to expect quantum confinement effect in this range. Other explanation relates the line to defects in the Si oxide/Si interface [21,22].

Peak *2* is the second order diffraction of the peak *0* as evidenced by a 780 nm long-wave-pass edge filter, this band disappeared if we used the filter. Band 2^* reflects the band—band recombination of crystalline silicon bulk materials. Both the crystalline core of the SiNWs and the substrate are able to give this emission. Peak *3* at 1270 nm with its sharp shape was also observed in the carbon-rich EFG (edge-defined film-fed growth) materials [23] and could be correlated to G-centers $(\mathrm{C}_i\mathrm{C}_s)$ near certain twin boundaries. Indeed, twins and other extended defects have been observed by TEM (transmission electron microscopy) within SiNWs [24]. However it should be noted that the G-line is only observed at low temperatures and disappears for temperature higher than 77 K. Peak 3^* at about 1320 nm is the second order diffraction of peak *1*.

Additional peak *4* appears at higher temperatures. Its intensity increases with increasing temperature. Fig. 4 shows the spectra taken at room tempareture with normal incidence of the beam to the sample (P) and cross section (X) after cleaving the sample. The difference between the two spectra may be due to the different area contributing to the emission. Peak *4* can be deconvoluted by two peaks positioned at 1420 and 1550 nm. They agree relatively well with the dislocation-related luminescence D2 and D1. This explanation is confirmed by photoluminescence (PL) measurement at 80 K shown in Fig. 5. The dislocation-

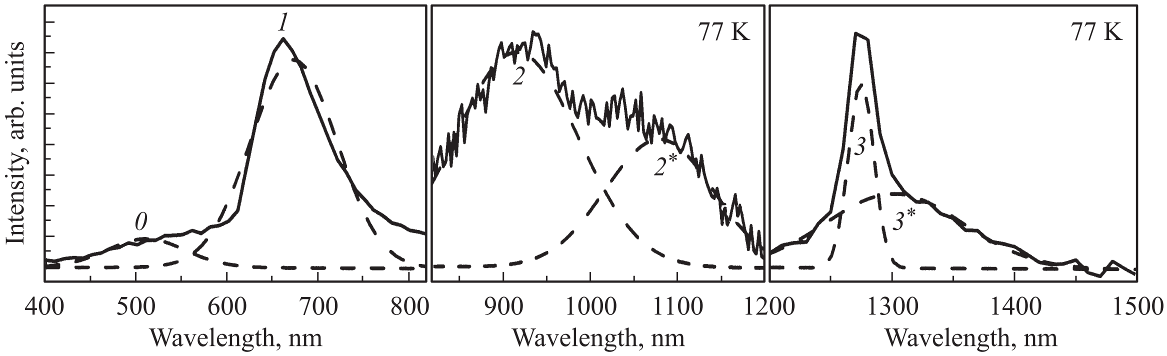

Figure 3. Details of the emission bands by Gaussian fit.

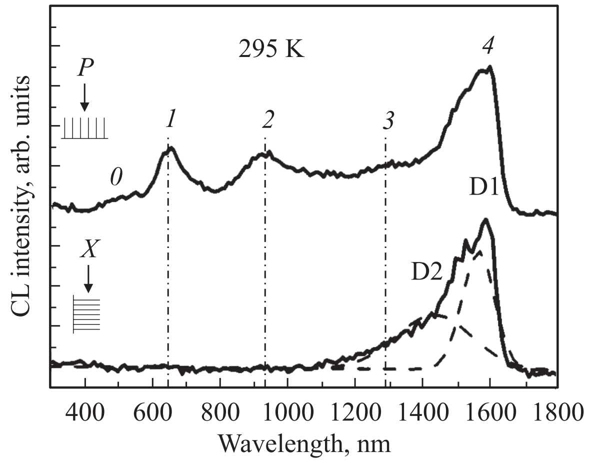

Figure 4. CL spectra taken at room temperature using normal incidence of beam current (P) and cross section (X) after cleaving of the sample. The dashed lines are the Gaussian fit of the spectrum X.

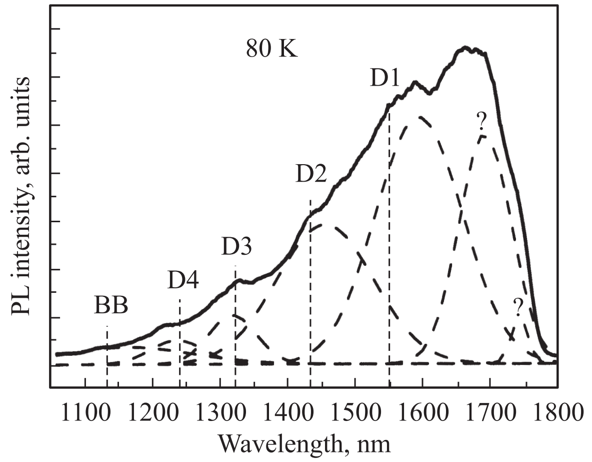

Figure 5. PL measurement of the SiNW at 80 K. The dashed lines are the deconvolution of the spectrum.

related D3 and D4 lines are observed at the same energies as in bulk material. D1 and D2 are shifted to higher wavelengths. The origins of the other two components at the higher wavelength side (see question marks) are not quite clear so far.

The reason why peak *4* appearing in the CL spectrum shown in Fig. 4 increases with increasing temperatures (anomalous temperature behaviour) remains still open. In dislocated bulk Si we observed an ordinary behaviour, i. e. decrease of the D1-line intensity with increasing temperature, see e. g. [25,26]. The anomalous temperature behaviour of peak *4* might be related to the fact that the confinement of the excess carriers in the SiNWs affects the efficiency of the different recombination channels as compared to bulk material.

Infrared emission around 1550 nm was also reported for nanocrystalline Si, namely for CVD grown nanocrystalline Si films [27] and for Si nanocrystals fabricated by mechanical milling of Si [28]. Within the nanocrystals a high density of extended defects was found by TEM in both types of samples, which may cause the observed infrared emission. Another possible factor, leading to enhanced D1 emission is oxygen accommodation within the extended defects [25].

5. Conclusion

In summary, we have investigated SiNWs by CL measurements, visible and infrared emissions were found and correlated to different mechanisms. Our results show that SiNWs are able to emit light in infrared range if they contain extended defects within the Si nanocrystalline core.

The author thanks Dr Winfried Seifert for his helpful discussions and critical read of the paper.

References

[1] R. Sauer, Ch. Kisielowski-Kemmerich, H. Alexander. Phys. Rev. Lett., **57**, 1472 (1986).
[2] H. Ennen, J. Schneider, G. Pomrenke, A. Axmann. Appl. Phys. Lett., **43**, 943 (1983).
[3] D. Leong, M. Harry, K.J. Reeson, K.P. Homewood. Nature, **387**, 686 (1997).
[4] L.T. Canham. Appl. Phys. Lett., **57**, 1046 (1990).
[5] Y.F. Zhang, Y.H. Tang, N. Wang, D.P. Yu, C.S. Lee, I. Bello, S.T. Lee. Appl. Phys. Lett., **72**, 1835 (1998).
[6] Y. Cui, L.J. Lauhon, M.S. Gudiksen, J. Wang. Appl. Phys. Lett., **78**, 2214 (2001).
[7] C. Wu, W. Qin, G. Qin, D. Zhao, J. Zhang, W. Xu, H. Lin. Chem. Phys. Lett., **378**, 368 (2003).
[8] Y. Wu, Y. Cui, L. Huynh, C.J. Barrelet, D.C. Bell, C.M. Lieber. Nano Lett., **4**, 433 (2004).
[9] S. Sharma, T.I. Kamins, M.S. Islam, R.S. Williams, A.F. Marshall. J. Cryst. Growth, **280**, 562 (2005).
[10] Y. Cui, X. Duan, J. Hu, C.M. Lieber. J. Phys. Chem. B, **104**, 5213 (2000).
[11] Y. Cui, Z. Zhong, D. Wang, W.U. Wang, C.M. Lieber. Nano Lett., **3**, 149 (2003).
[12] J. Niu, J. Sha, D. Yang. Physica E, **23**, 131 (2004).
[13] D.D. Ma, S.T. Lee, J. Shinar. Appl. Phys. Lett., **87**, 033 107 (2005).
[14] N. Wang, Y.H. Tang, Y.F. Zhang, C.S. Lee, S.T. Lee. Phys. Rev. B, **58**, 16 024 (1998).
[15] M.A. Stevens Kalceff, M.R. Phillips. Phys. Rev. B, **52**, 3122 (1995).
[16] M.V. Zamoryanskaya, V.I. Sokolov, A.A. Sitnikova, S.G. Konnikov. Sol. St. Phenomena, **63–64**, 237 (1998).
[17] Roushdey Salh, A von Czarnowski, H.-J. Fitting. Phys. Status Solidi C, **2**, 580 (2005).
[18] H. Nishikawa, R.E. Stahlbush, J.H. Stathis. Phys. Rev. B, **60**, 15 910 (1999).
[19] T. Suzuki, L. Skuja, K. Kajihama, M. Hirano, T. Kamiya, H. Hosono. Phys. Rev. Lett., **90**, 186 404 (2003).
[20] B. Delly, E.F. Steigmeier. Appl. Phys. Lett., **67**, 16 (1995).

[21] X.H. Sun, N.B. Wong, C.P. Li, S.T. Lee, T.K. Sham. J. Appl. Phys., **96**, 3447 (2004).
[22] D.D. Ma, S.T. Lee, J. Shinar. Appl. Phys. Lett., **87**, 033 107 (2005).
[23] K.D. Vernon-Parry, G. Davies, S. Galloway. Semicond. Sci. Technol., **20**, 171 (2005).
[24] N. Wang, Y.H. Tang, Y.F. Zhang, C.S. Lee, S.T. Lee. Phys. Rev. B, **58**, 16 024 (1998).
[25] M. Kittler, M. Reiche, T. Arguirov, W. Seifert, X. Yu. Phys. Status Solidi A, **203**, 802 (2006).
[26] I. Matsubara, S. Sasahara, T. Mishina, Y. Ishibashi, T. Kobayashi, J. Nakahara. Phys. Status Solidi B, **243**, 1893 (2006).
[27] S. Binetti, M. Acciarri, M. Bollani, L. Fumagalli, H. von Känel, S. Pizzini. Thin Sol. Films, **487**, 19 (2005).
[28] C. Díaz-Guerra, A. Montone, J. Piqueras, F. Cardellini. Sol. St. Phenomena, **78**–**79**, 103 (2001).

Редактор Л.В. Шаронова